GROWTH OF SILICON NANOWIRES BY THERMAL ANNEALING OF THICK GOLD CATALYTIC LAYER ON SILICON SUBSTRATE UNDER DIFFERENT ATMOSPHERES

ŠPERKA Jiří[1], JAŠEK Ondřej[1,2] ZAJÍĆKOVÁ Lenka[1,2], HAVEL Josef[2]

[1]Masaryk University, The Central European Institute of Technology (CEITEC), Brno, Czech Republic, EU
[2]Masaryk University, Faculty of Science, Brno, Czech Republic, EU

Abstract

Silicon nanowires (Si NWs) were grown from Si wafer upon thermal annealing in the presence of catalytic gold layer. The Si substrate coated with 100 nm thick Au sputtered layer was thermally annealed at 1000 °C for 60 min in argon and hydrogen atmosphere at 8 kPa. The influence of argon and hydrogen atmospheres on the growth of Si NWs was investigated. It was found that by using the hydrogen atmosphere we were able to grow Si NWs, while the growth in argon atmosphere was sporadic. The catalytic layer morphology and composition were examined using atomic force microscopy and laser desorption-ionization time of flight mass spectrometry, while nanowire structure was observed through scanning electron microscope and energy dispersive X-ray spectroscopy.

Keywords: Nanowires, Silicon, Gold, Eutectics, Surface processes.

1. INTRODUCTION

Nanotubes and nanowires are widely studied nanostructures in the field of basic and applied research. Among nanowires, silicon nanowires have many possible applications in electronics, such as solar cells or lithium battery anodes. Several methods of Si NWs growth have been reported since the first publication on their growth was published [1]. Si NWs can be fabricated through both 'top-down' and 'bottom-up' approaches. Si NWs have been already successfully grown by chemical vapor deposition (CVD) using various catalysts under different atmospheres depending on the process [2]. We have shown in our previous publications [3, 4] that growth of nanostructures is strongly influenced by catalyst thickness and deposition parameters such as hydrogen content. These effects, such as size of precursor nanoparticles and their distribution, are very strong not just during the growth but especially during annealing phase before deposition [5]. Growth of Si NWs have been studied using silane (SiH4) diluted in hydrogen and gold as the catalyst [6, 7, 8]. Epitaxial growth of Al-catalyzed Si NWs was studied via a vapor-solid-solid (VSS) mechanism in silane/argon gas mixture [9]. Disilane/helium gas mixtures with gold catalyst have been used for the Si NWs growth, too [10]. The Si-free atmospheres can be also suitable for the growth, if hydrogen etches exposed silicon regions to provide silyl radicals in the vapor phase [11]. This effect results in CVD-like mode. The most frequently used catalyst for Si NWs growth is gold in the form of thin catalytic layer, several nanometers. The Au-Si phase diagram is the eutectic type with the eutectic temperature of 363 °C and the eutectic composition of 19 % Si [12]. The heating of silicon covered by gold to the temperatures above the eutectic point resulted in the formation of Au-Si alloy. Small Au-Si droplets are formed instead of a homogenous layer during further annealing. Larger droplets grow at the expense of smaller, an effect known as Ostwald ripening [13].

In this paper, we focus on Si NWs growth from Si wafer upon thermal annealing in the presence of thick catalytic gold layer.

2. EXPERIMENTAL

2.1. Preparation of gold catalytic layer

The gold catalytic layer, with the thickness of 100 nm, was prepared by magnetron sputtering (Bal-Tec Sputter Coater SCD 050, gold target purity 99.99 %) on Si (100) wafer (51 mm in diameter and 0.28 mm in thickness).

Before loading into the sputter-deposition chamber, the silicon substrate was cleaned with ethanol in an ultrasonic bath and dried with a nitrogen flow. The gold-coated silicon wafer was broken into 10 × 10 mm squares that were used for the growth of nanowires.

2.2. Synthesis of nanowires by thermal annealing

The thermal synthesis of Si NWs proceeded in the centre of horizontal furnace which consists of quartz glass tube (1 m long, inner diameter 45 mm and hot zone length of 150 mm) terminated with flanges The temperature inside the furnace was measured by the type S thermocouple. The gas flow rate was controlled by electronic flow meter and the whole system was evacuated by a rotary pump. The annealing was done in the following sequence. The whole experimental setup was at first evacuated to avoid the air impurities during the annealing (ultimate pressure 5 Pa) and the quartz tube was purged for 5 min in advance with chosen gas (hydrogen or argon). During the annealing and cooling, the gas flow rate was kept constant 220 sccm corresponding to 8 kPa pressure in the furnace. The temperature was continuously increased up to 1000 °C in 25 °C/min rate. After reaching the maximum temperature the chamber was held at 1000 °C for 60 min. After the annealing, the furnace was cooled down to room temperature in about 5 hours with exponential temperature decay.

2.3. Characterization techniques

Synthesized nanostructures were characterized using scanning electron microscopy (TESCAN MIRA3) to study the morphology and structure. Energy-dispersive X-ray spectroscopy analysis (Oxford Instruments) on the micro-scope was employed to reveal the chemical composition of the structures. Curved field reflectron time-of-flight mass spectrometer (CFR TOF MS, AXIMA, Kratos Analytical, Manchester, UK) equipped with a nitrogen laser (337 nm) from Laser Science Inc. (Franklin, MA, USA) was used to acquire mass spectra of gold catalytic layer before annealing. The repetition modes of experiments were performed at a frequency of 10 Hz and a pulse time width of 3 ns. The laser fluency was 60 mJ per pulse and maximum laser power was 20 mW while the irradiated spot size was ~150 μm in diameter. Mass spectra in laser desorption ionization (LDI) mode i.e. without any matrix were measured after the pressure dropped below 10^{-4} Pa. Positive ion spectra were recorded either in linear or reflectron modes from at least 50 laser shots [19]. Internal mass calibration was done in both ionization modes using gold clusters. The roughness of gold catalytic layer has been evaluated using Thermomicroscopes Autoprobe CP Research Atomic Force Microscope on square area with dimensions of 30 × 30 μm.

3. RESULTS AND DISCUSSION

3.1. Composition and morphology of sputtered gold catalytic layer

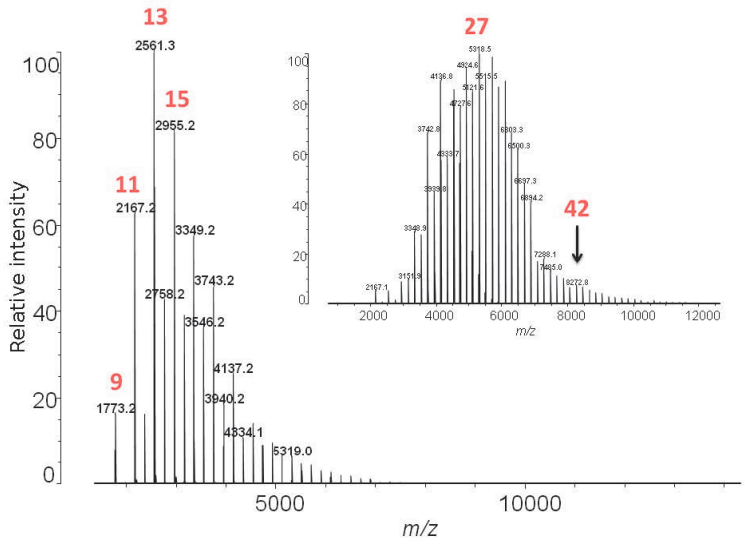

Fig. 1 Example of LDI mass spectra in two mass ranges as generated from gold catalytic layer showing formation of gold clusters. The integer numbers indicate the number of gold atoms in Au^+ clusters

Although, the gold purity should be simply related to the target composition (purity 99.99 %) in the sputter tool, the LDI-TOF mass spectroscopy was employed in order to verify the purity of gold catalytic layer. A limited number of pulses (50) dispersed in raster was used in order not to ablate gold layer and avoid the penetration to the silicon substrate. LDI-TOF mass spectra showed that via laser ablation of the sputtered catalytic gold layer only gold clusters Au_m (m=1-50) were generated and no contamination has been found except sodium and potassium as common impurities. An example of mass spectra demonstrating the presence of pure gold clusters is given in **Fig. 1**. The roughness of the sputtered gold layer on the silicon substrate was obtained by using the AFM and evaluated by Gwyddion software [20]. Calculated root mean square surface roughness was 1.6 nm.

3.2. Surface morphologies after thermal annealing in different atmospheres

No droplets or wires were observed after annealing in vacuum. Large Au-Si droplets with mean diameter of approximately 8 μm and of various shapes were created under argon atmosphere (**Fig. 2a**). The annealing in the hydrogen atmosphere led to the growth of smaller Au-Si droplets with the mean diameter of approximately 5 μm and even smaller, tens of nanometers, droplets were also found on the substrate (**Fig. 3a**). The surface area EDX scan (**Fig. 4**) together with the EDX elemental analysis at three different spots (**Fig. 2b**) of the sample annealed in argon reveals that the small droplets are mostly composed of gold, silicon and oxygen. The elemental surface composition on the sample at various places differs considerably. Small content of gold was found in the droplet-free places (**Table 1**).

Table 1 Elemental composition obtained by EDX analysis at three different places on the sample annealed in argon (**Fig. 2**b)

Spot	Au [%]	Si [%]	O [%]	C [%]
1 (spectrum 3)	84	5	8	3
2 (spectrum 4)	0.4	87	8	4
3 (spectrum 5)	1	84	10	4

The surface area EDX scan (**Fig. 5**) performed on the surface on layer annealed in hydrogen confirms that the droplet is composed mainly of Au with small amount of silicon. Oxygen signal suggests that there could be some reaction of Si with residual oxygen during or after annealing and possible oxidation of Au-Si droplet [8, 18] and we cannot exclude possibility that the nanowires are partially composed of silicon oxide.

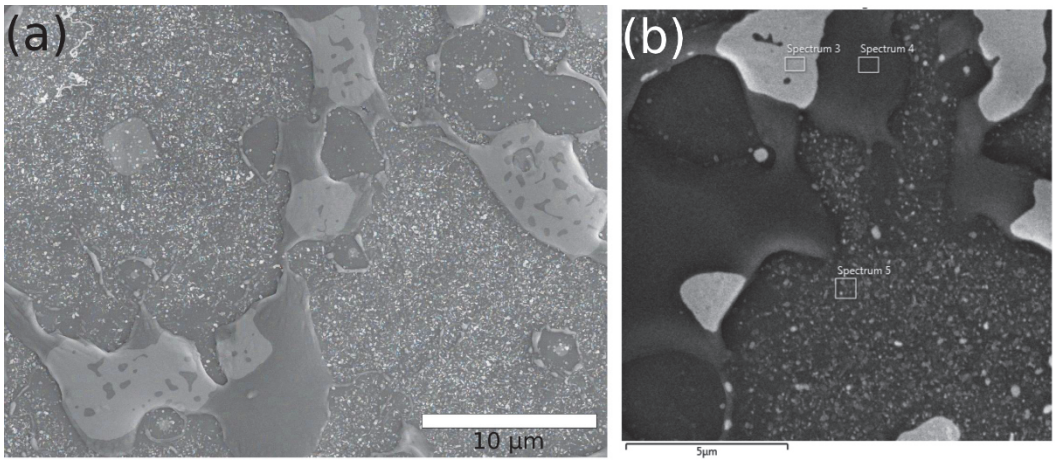

Fig. 2 Gold layer on Si after 60 min annealing in argon at 1000 ◦C. (a) Overview SEM image (SE mode). (b) Image with highlighted spots which were used for EDX analysis

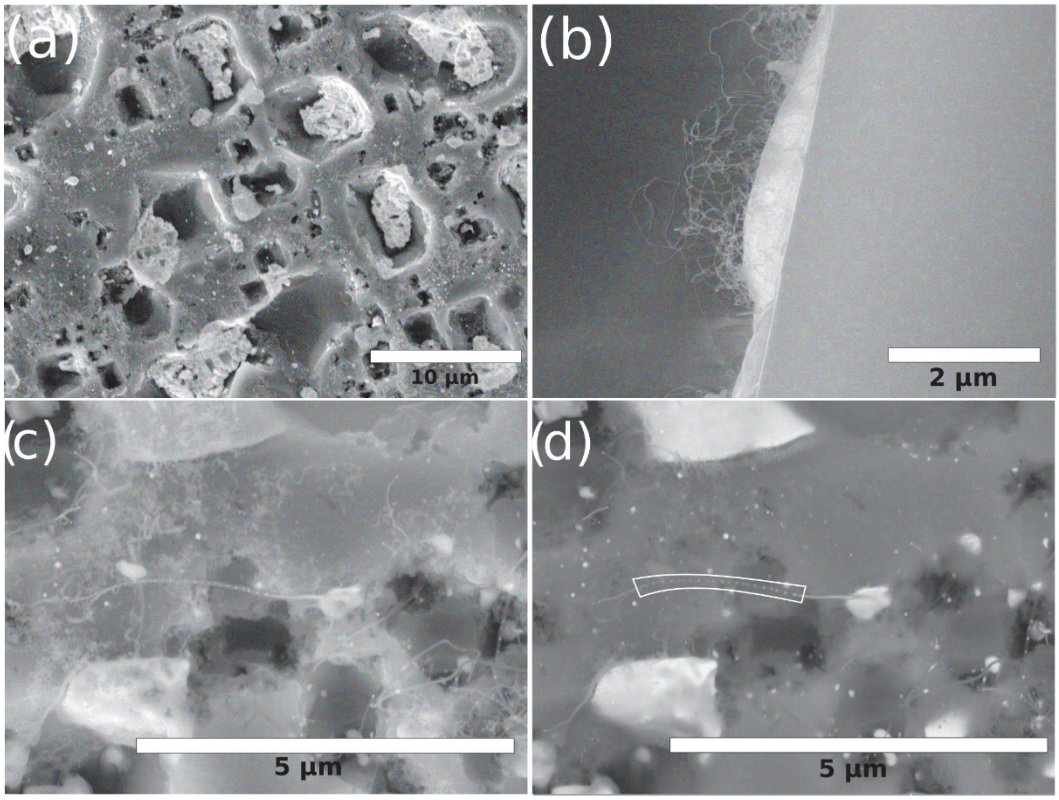

Fig. 3 Gold layer on Si after 60 min annealing in hydrogen at 1000 ◦C. (a) Overview SEM image (SE mode). (b) Cross section of broken sample with Si NWs (SE mode). (c) Low magnification image (SE mode). (d) BSE image with highlighted embedded gold nanoparticles inside Si NW.

3.3. Properties of grown silicon nanowires and influence of gas atmosphere on their synthesis

There was no growth of Si NWs under vacuum. On the contrary, the sample annealed in argon exhibited small amount of randomly distributed Si NWs, which detailed analysis has revealed. Dense curved Si NWs were found on the sample after hydrogen annealing (**Fig. 3b**). The length of the Si NWs is up to several micrometers, while the diameter ranges from 20 nm to 100 nm. The growth of the Si NWs proceeds from the smaller Au-Si-O droplets as can be found on the **Fig. 3c**. Similar effect was already observed and explained in the case of the annealing in argon atmosphere [18]. It was described that the super saturation is directly related to the diameter of the Au-Si-O droplet and determines the growth of Si NWs. Small gold nanoparticles with diameter of around 20 nm (**Fig. 3d**) have been observed uniformly encapsulated in bulk of some Si NWs.

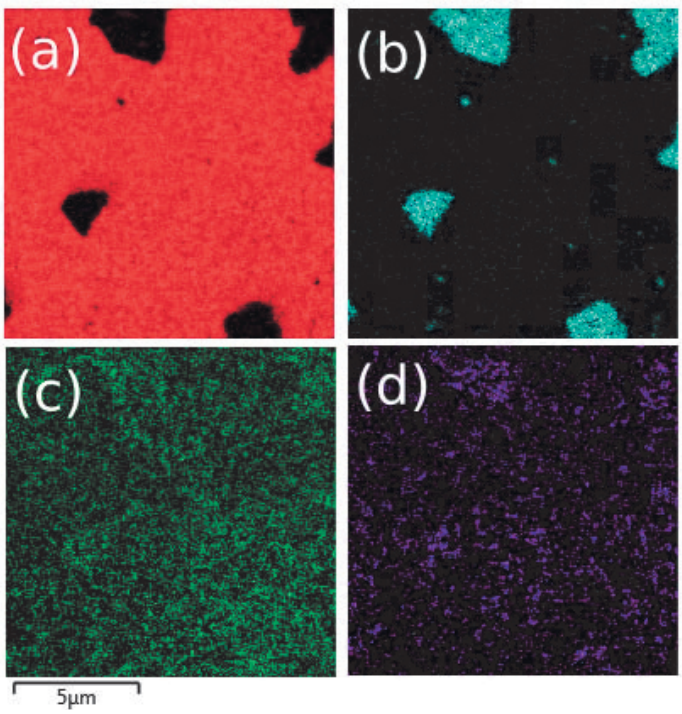

Fig. 4 EDX-SEM surface mapping after annealing in argon: (a) Si, (b) Au, (c) O, (d) C

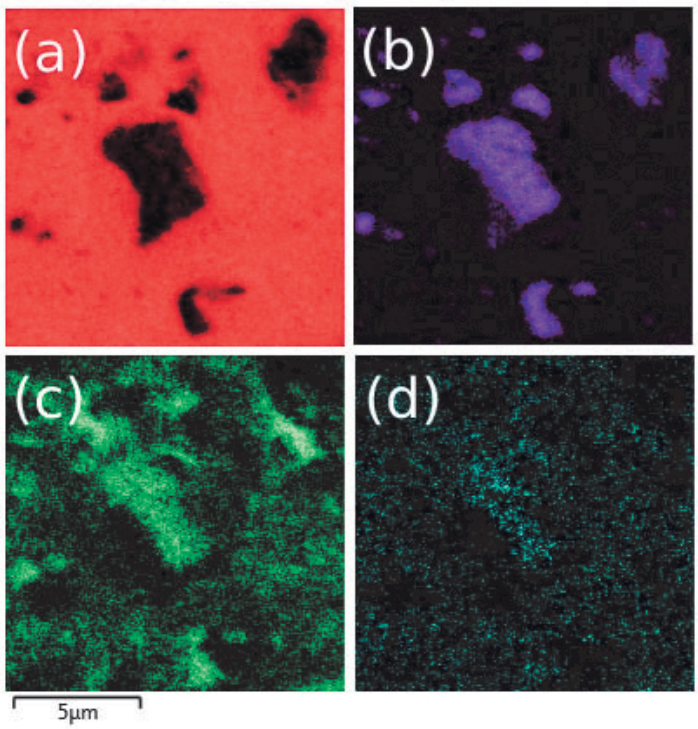

Fig. 5 EDX-SEM surface mapping after annealing in hydrogen: (a) Si, (b) Au, (c) O, (d) C

This entrapping of smaller Au nanoparticles is considered to be resulted from the super saturation of Au and SiOx [18]. The Si NWs growth in hydrogen atmosphere can be explained as follows: Reactive hydrogen heated to 1000 °C can react with solid silicon and locally create various silicon compounds, so the growth can proceed like during standard CVD [13]. This can be one reason for rapid growth of Si NWs in hydrogen atmosphere and slower growth in argon. Another aspect is local cooling of the surface. The overcooling is critical to initiate the preferential unidirectional nanowire growth [18]. The cooling depends on thermal conductivity of gas used. Hydrogen has approximately ten times higher thermal conductivity than argon which can be another reason of different rate of Si NWs growth in these two gases.

4. CONCLUSIONS

We investigated the Si NWs growth in argon and hydrogen (at pressure of 8 kPa) during one hour long thermal annealing (1000 °C) of 100nm thick gold catalytic layer deposited on silicon. During the annealing, the gold layer reconstructs and forms together with silicon droplets with various diameters. The size of the droplets strongly depends on the gas atmosphere. The significant growth of nanowires, from 100 nm thick gold layer, was observed after annealing in hydrogen, but not in argon. This can be explained by different reactivity and thermal conductivity of these gases.

ACKNOWLEDGEMENTS

This work was supported by CEITEC - Central European Institute of Technology CZ.1.05/1.1.00/02.0068 and R&D Center for Low-Cost Plasma and Nanotechnology Surface Modications CZ.1.05/2.1.00/03.0086 funded by European Regional Development Funds project and LO1411 (NPU I) funded by Ministry of Education Youth and Sports of Czech Republic.

REFERENCES

[1] TREUTING R., ARNOLD S., Orientation habits of metal whiskers, Acta Metallurgica, Vol. 5, 1957, pp. 598.

[2] SCHMIDT V., WITTEMANN J., GöSELE U., Growth, thermodynamics, and electrical properties of silicon nanowires, Chemical reviews, Vol. 110, 2010, pp. 361-388.

[3] ZAJICKOVA L., JASEK O., ELIAS M., SYNEK P., LAZAR L., SCHNEEWEISS O., HANZLIKOVA R., Synthesis of carbon nanotubes by plasma-enhanced chemical vapor deposition in an atmospheric-pressure microwave torch, Pure and Applied Chemistry, Vol. 82, 2010, pp. 1259-1272.

[4] JASEK O., ELIAS M., ZAJICKOVA L., KUCEROVA Z., MATEJKOVA J., REK. A., BURSIK J., Discussion of important factors in deposition of carbon nanotubes by atmospheric pressure microwave plasma torch, Journal of Physics and Chemistry of Solids, Vol. 67, 2007, pp. 738-743.

[5] PISANA S., CANTORO M., PARVEZ A., HOFMANN S., FERRARI A.C., ROBERTSON J., The role of precursor gases on the surface restructuring of catalyst films during carbon nanotube growth, Physica E, Vol. 37, 2007, pp. 1-5.

[6] TIAN B. , ZHENG X., KEMPA T. J., FANG Y., YU N., YU G., HUANG J., LIEBER C. M. Lieber, Coaxial silicon nanowires as solar cells and nanoelectronic power sources, Nature , Vol. 449, 2007, pp. 885-889.

[7] WU Y., CUI Y., GUYNH L., BARRELET C. J., BELL D. C., LIEBER C. M., Controlled growth and structures of molecular-scale silicon nanowires, Nano Letters, Vol. 4, 2004, pp. 433-436.

[8] ZENG X., XU Y., ZHANG S., HU Z., DIAO H., WANG Y., KONG G., LIAO X., Silicon nanowires grown on a pre-annealed Si substrate, Journal of crystal growth, Vol. 247, 2003, pp. 13-16.

[9] WANG Y., SCHMIDT V., SENZ S., GÖSELE U., Epitaxial growth of silicon nanowires using an aluminium catalyst, Nature nanotechnology, Vol. 1, 2006, pp. 186-189.

[10] HANNON J., KODAMBAKA S., ROSS F., TROMP R., The influence of the surface migration of gold on the growth of silicon nanowires, Nature, Vol. 440, 2006, pp. 69-71.

[11] SUNKARA M. K., SHARMA S. MIRANDA R., LIAN G., DICKEY E., Bulk synthesis of silicon nanowires using a low-temperature vapor-liquid-solid method, Applied Physics Letters, Vol. 79, 2001, pp. 1546-1548.

[12] ANATATMULA R., JOHNSON A., GUPTA S., HORYLEV R., The gold-silicon phase diagram, Journal of Electronic Materials, Vol. 4. 1975, pp. 445-463.

[13] SCHMIDT V., WITTERMAN J. V., SENZ S. , GöSELE U. , Silicon nanowires: A review on aspects of their growth and their electrical properties, Advanced Materials, Vol. 21, 2009 pp. 2681-2702.

[14] WAGNER R., ELLIS W. , Vapor-liquid-solid mechanism of single crystal growth, Applied Physics Letters, Vol. 4, 1964, pp. 89-90.

[15] WANG H., ZEPEDA-RUIZ L. A., GILMER G. H., UPMANYU M., Atomistic of vapour-liquid-solid nanowire growth, Nature communications, Vol. 4, 2013, pp. 1956.

[16] PARK W. I., ZHENG G., JIANG X., TIAN B., LIEBER C. M., Controlled synthesis of millimeter-long silicon nanowires with uniform electronic properties, Nano Letters, Vol. 8, 2008, pp. 3004-3009.

[17] BANDARU P., PICHANUSAKORN P. , An outline of the synthesis and properties of silicon nanowires, Semiconductor science and technology, Vol. 25, 2010, pp. 024003.

[18] LI F. J., ZHANG S., Lee J.-W., ZHAO D. Zhao, Wire or no wire -depends on the catalyst layer thickness, Journal of Crystal Growth, Vol. 381, 2013, 87-92.

[19] BURŠÍKOVÁ V., ŘEHULKA P., CHMELÍK J., ALBERTI M., ŠPALT Z., JANČA J., HAVEL J., Laser ablation time-of-flight mass spectrometry (la-tof-ms) of “nitrogen doped diamond-like carbon (dln) nano-layers”, Journal of Physics and Chemistry of Solids, Vol. 68, 2007, pp. 701-706.

[20] NEČAS D. , KLAPETEK P., Gwyddion: an open-source software for SPM data analysis, Central European Journal of Physics, Vol. 10, 2012, pp. 181-188.